Recent results from LHCb
PDF4LHC meeting

Marek Sirendi
on behalf of the LHCb collaboration

University of Cambridge

October 27, 2015

Recent results from LHCb

Measurement of the forward Z boson production cross-section in pp collisions at $\sqrt{s} = 7\,\mathrm{TeV}$

JHEP08(2015)039 arXiv:1505.07024

Measurement of the forward W and Z boson production cross-sections in pp collisions at $\sqrt{s} = 8\,\mathrm{TeV}$

NEW

LHCb-PAPER-2015-049

Measurement of the forward-backward asymmetry in $Z/\gamma^* \to \mu^+\mu^-$ decays and determination of the effective weak mixing angle

arXiv:1509.07645

First observation of top quark production in the forward region

Phys.Rev.Lett. 115,112001(2015) arXiv:1506.00903

Measurement of the exclusive Υ production cross-section in pp collisions at $\sqrt{s} = 7\,\mathrm{TeV}$ and $8\,\mathrm{TeV}$

JHEP09(2015)084 arXiv:1505.08139

LHCb detector

arXiv:1504.07670 | arXiv:1412.6352 | JINST3 (2008) S08005

- Single arm spectrometer optimised for the study of B and D decays;
- Limited to $\sim 4\%$ of the solid angle;
- Corresponds to $2 < \eta < 5$, $\eta \equiv -\ln\left[\tan\left(\frac{\theta}{2}\right)\right] \approx y$;
- The uncertainty on $\mathscr{L}$ is 1.7% (7 TeV) and 1.2% (8 TeV).

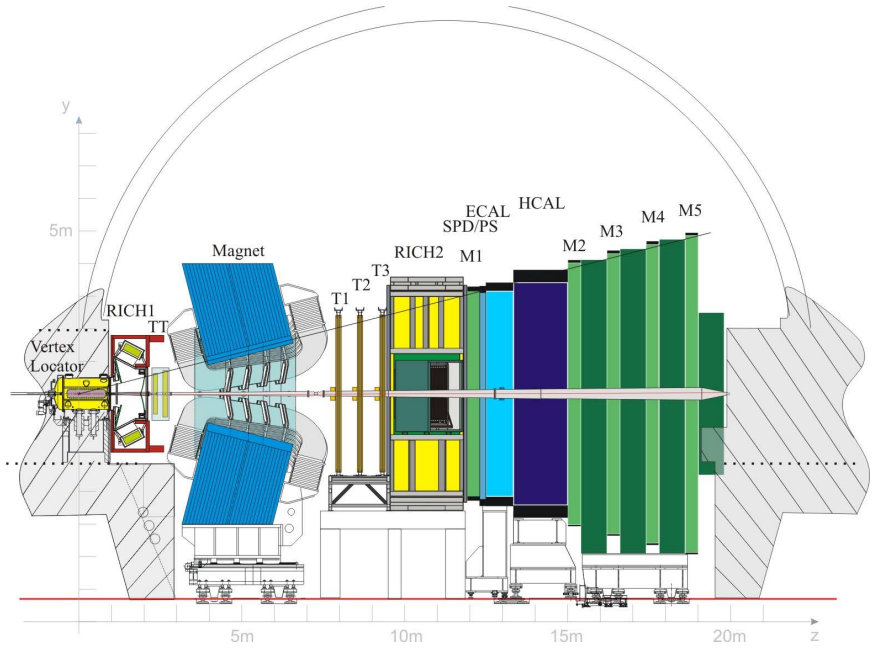

- $\frac{\Delta p}{p} = 0.4\%@5\,\mathrm{GeV}$ and $0.6\%@100\,\mathrm{GeV}$;
- $\sigma(IP) = 20\mu\mathrm{m}$;
- $\epsilon_{track} > 96\%$;
- $\epsilon_{PID}(\mu) \sim 97\%$ with MisID$(\pi \to \mu) \sim 1-3\%$.

Motivation

Motivation

arXiv:0808.1847

Electroweak measurements in the forward region

- probe pQCD and electroweak theory in a novel region of (x, Q^2) phase space;
- constrain PDFs at low x and high Q^2.

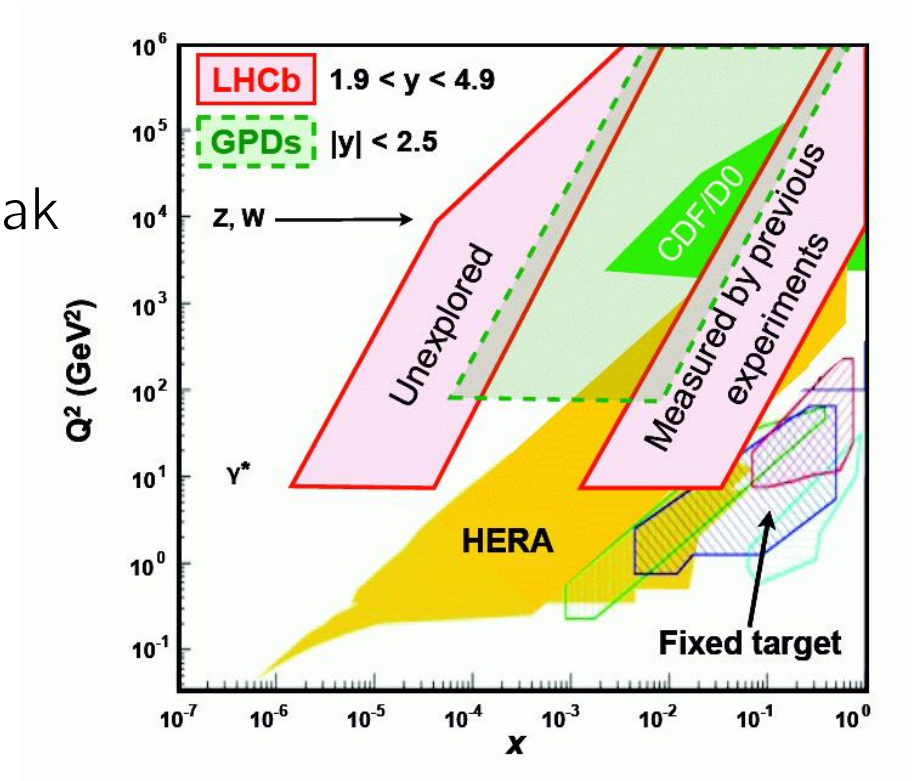

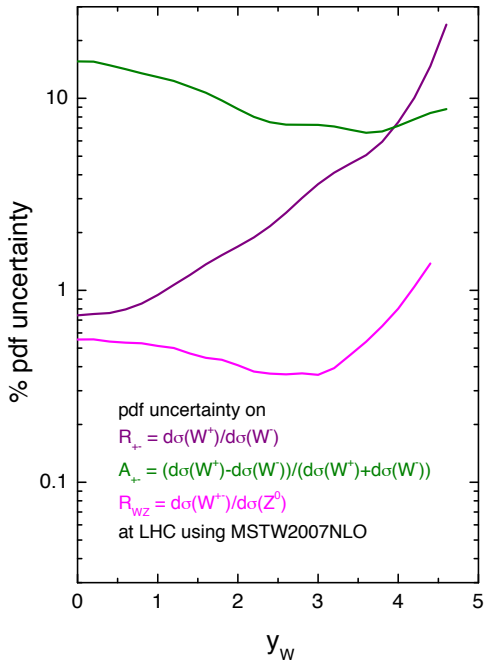

- PDF uncertainties become particularly large at forward rapidities (Thorne et al.);
- LHCb ideally placed to contribute.

Motivation – NNPDF3.0

arXiv:1410.8849

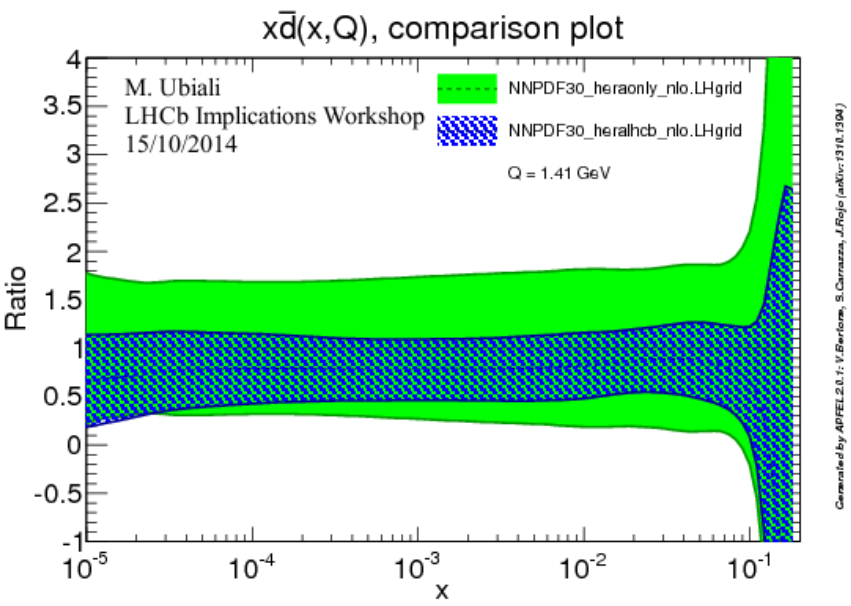

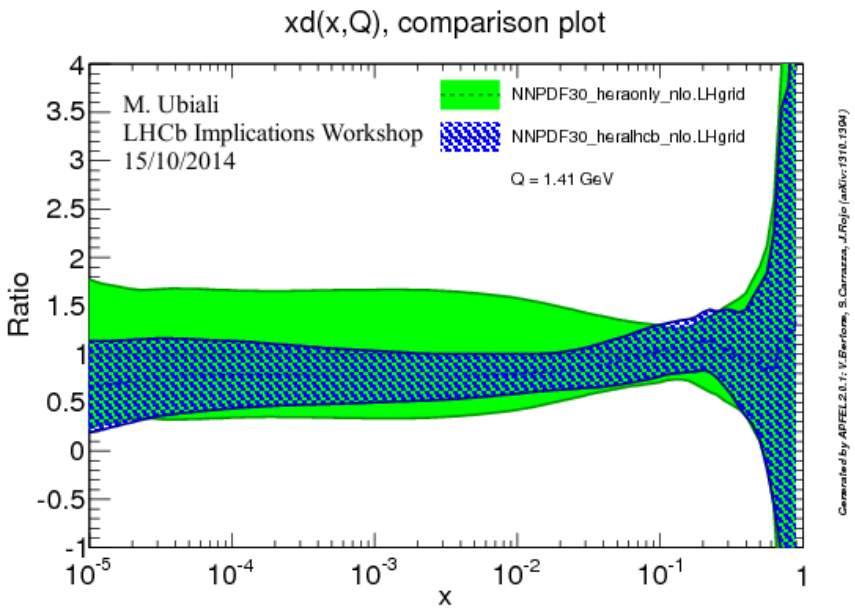

The impact of our early ($37\,\mathrm{pb}^{-1}$) $W \to \mu\nu$ (JHEP06 (2012) 58) and $Z \to ee$ (JHEP02 (2013) 106) measurements is clearly visible.

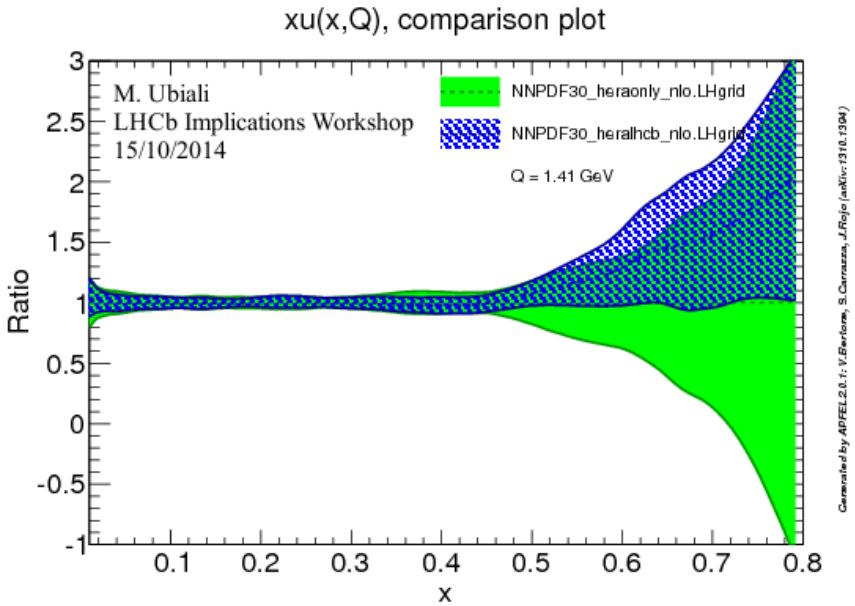

Results

Inclusive Z @ $7\,\mathrm{TeV}$ – results

JHEP08(2015)039

$\sigma_{Z\to\mu^+\mu^-}$ cross-section at $7\,\mathrm{TeV}$ is measured to be

$$\sigma_{Z\to\mu^+\mu^-} = 76.0 \pm 0.3\,(stat.) \pm 0.5\,(syst.) \pm 1.0\,(beam) \pm 1.3\,(lumi.)\mathrm{pb}$$

- Results are given at Born-level;
- Theory prediction is from FEWZ at NNLO;
- A selection of NNLO PDF sets are used;
- Results are consistent with the measurement of $Z \to ee$ and $Z \to \tau\tau$.

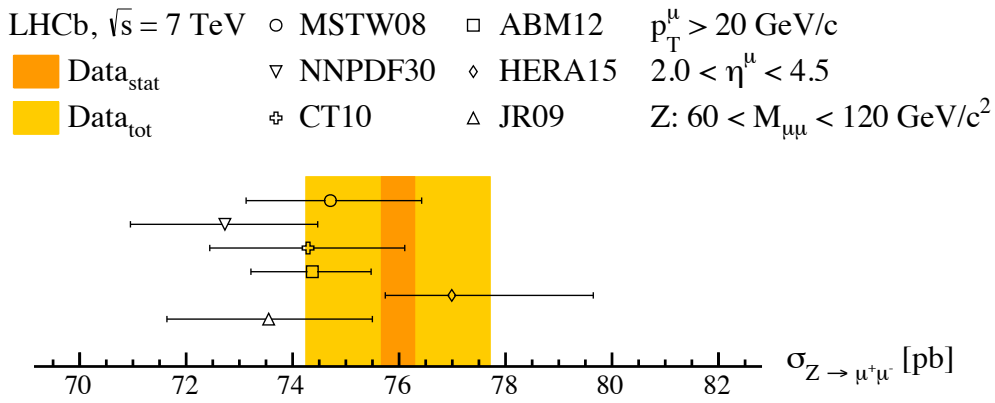

$$p_{\mathrm{T}}^{\mu} > 20\,\mathrm{GeV}$$
$$2.0 < \eta^{\mu} < 4.5$$
$$60 < M_{\mu\mu} < 120\,\mathrm{GeV}$$

Inclusive Z @ $7\,\mathrm{TeV}$ differential cross-sections

JHEP08(2015)039

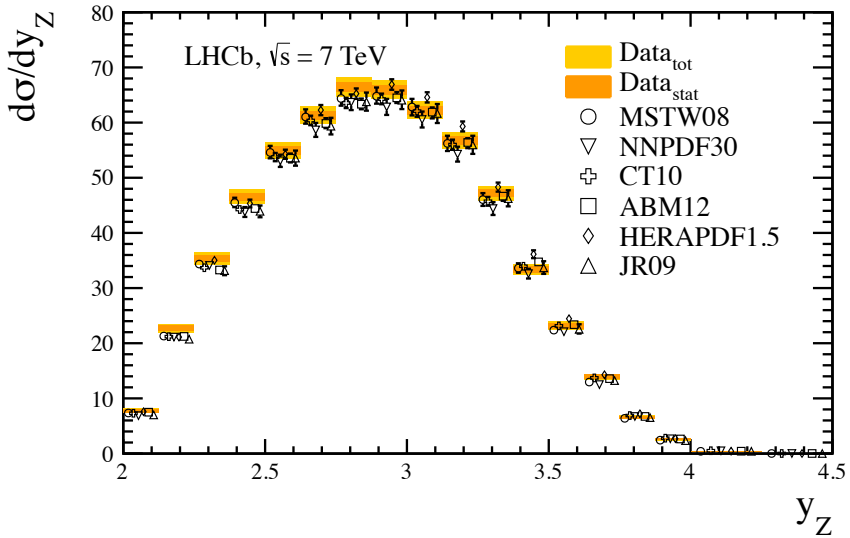

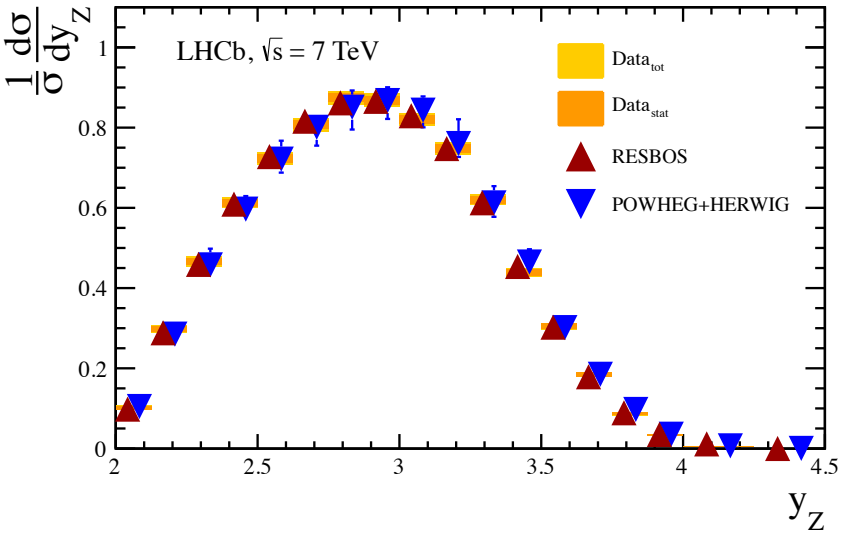

The measured cross-sections are in agreement with NNLO predictions using different PDF sets. Correlation matrices are provided.

Inclusive W analysis strategy

JHEP08(2015)039

JHEP12 (2014) 079

- The signal yield is determined from a fit to p_{T}^{μ};
- Signal and electroweak templates are taken from simulation;
- The decay in flight, $K/\pi \to \mu\nu$, component floats freely in the fit with a template determined from data;
- Purities are determined to be $\sim 77\%$.

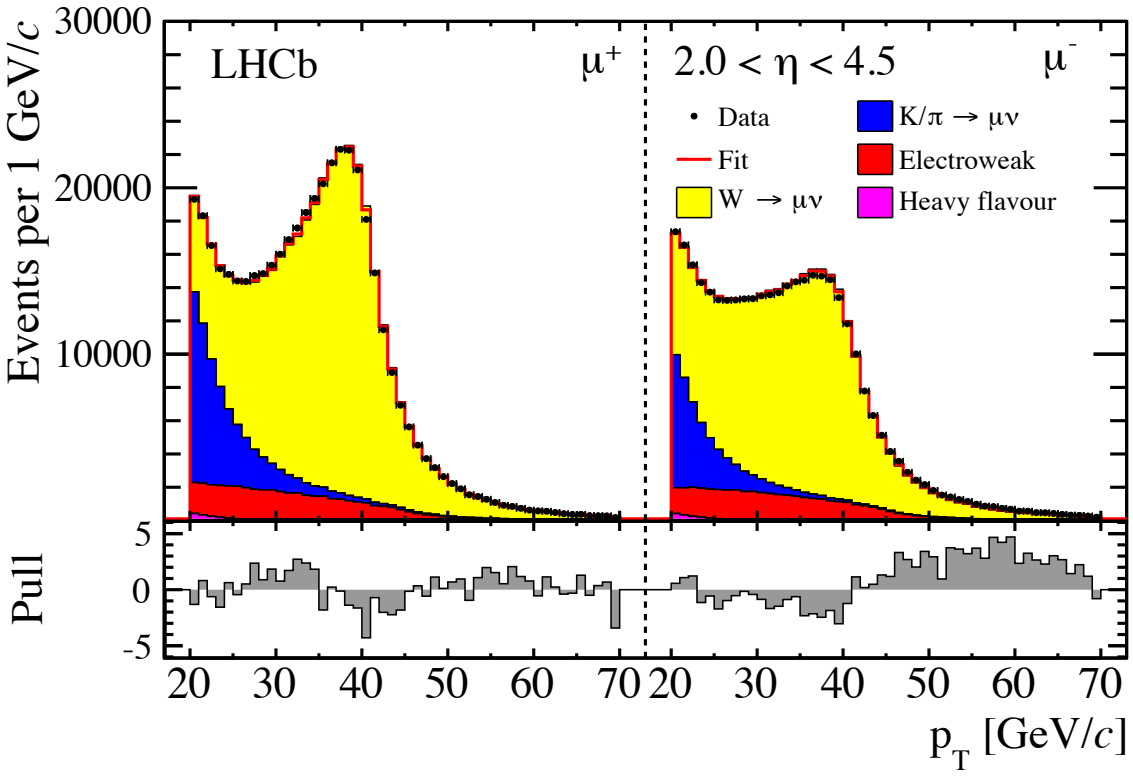

Inclusive W and Z @ 7 TeV

JHEP08(2015)039

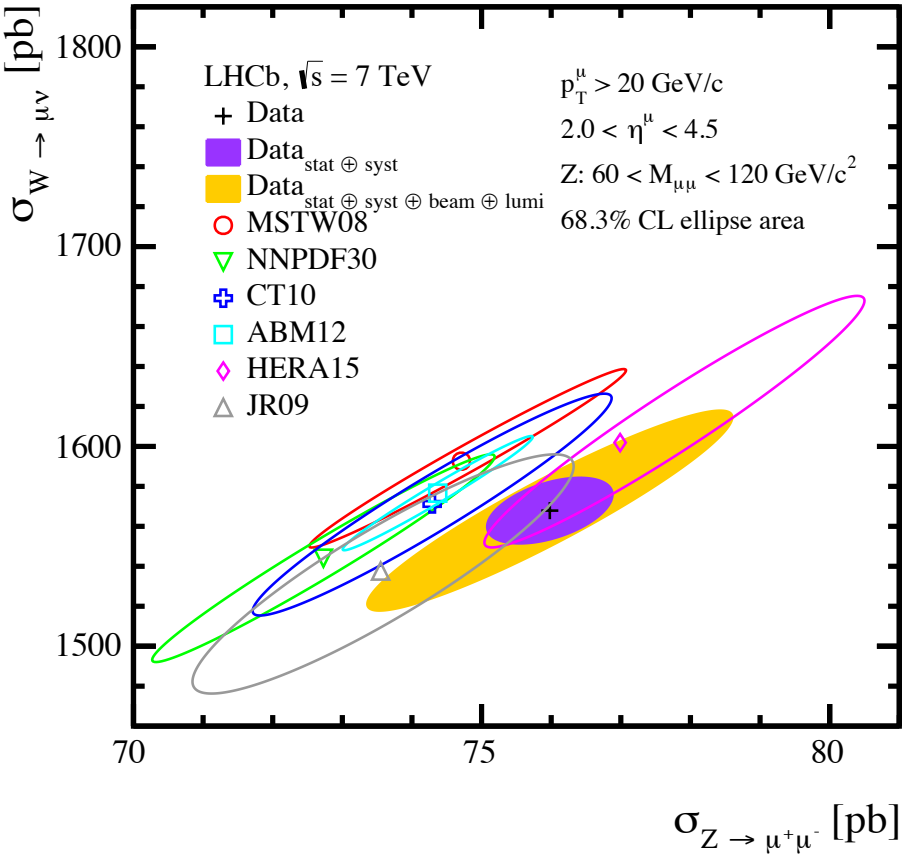

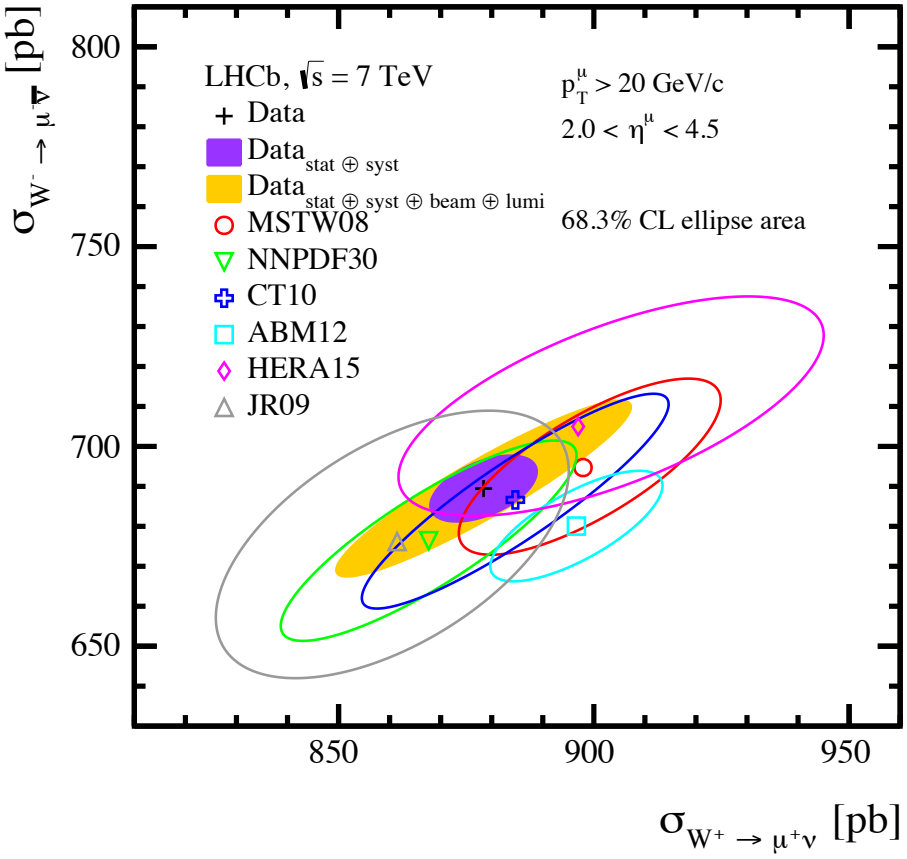

W and Z ratios @ 7 TeV

JHEP08(2015)039

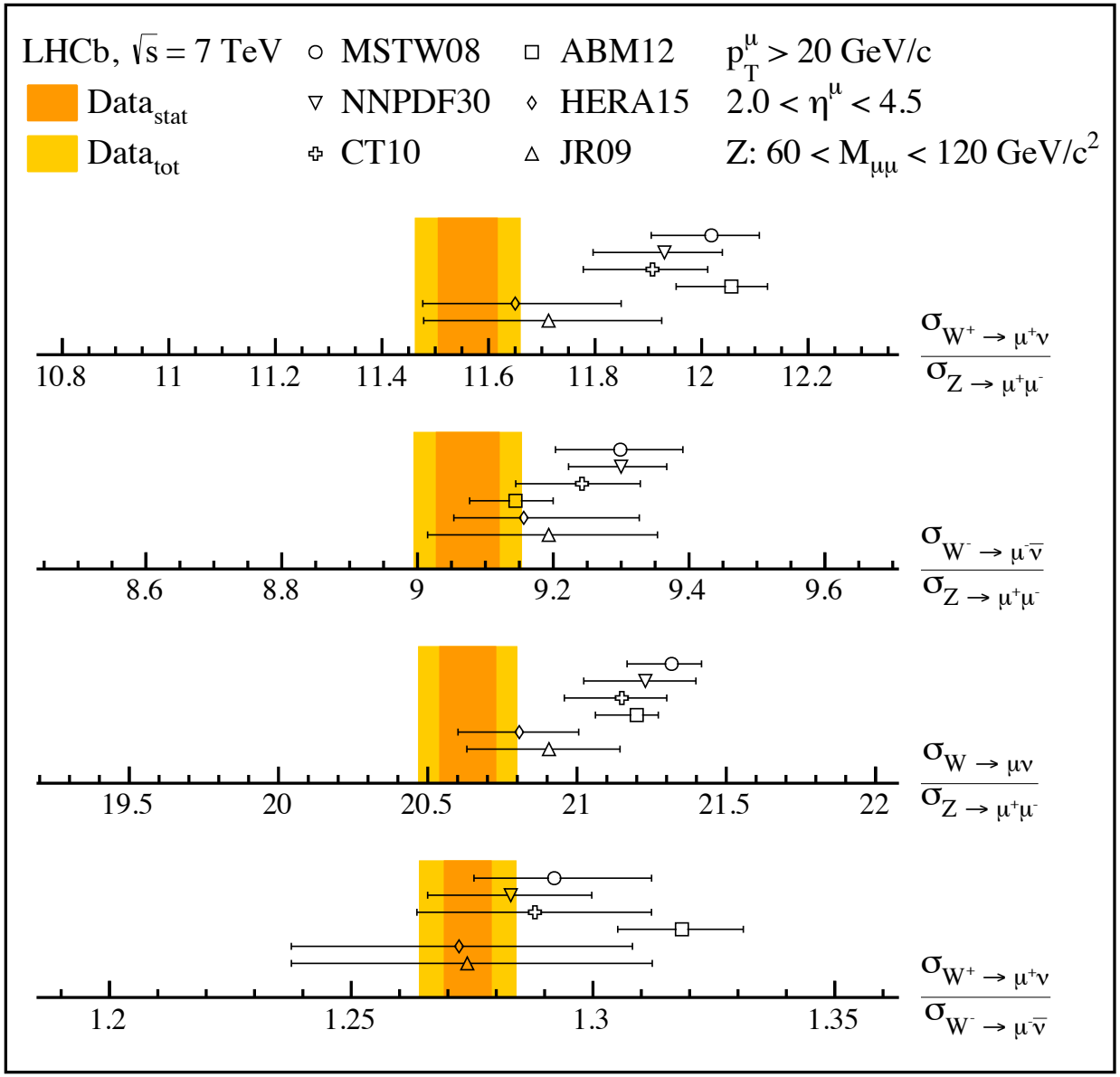

Inclusive W and Z @ $8\,\mathrm{TeV}$– results

LHCb-PAPER-2015-049

The W and Z cross-sections at $8\,\mathrm{TeV}$ are measured to be

$$\sigma_{Z\to\mu^+\mu^-} = 95.0 \pm 0.3\,(stat.) \pm 0.7\,(syst.) \pm 1.1\,(beam) \pm 1.1\,(lumi.)pb$$

$$\sigma_{W^+\to\mu^+\nu} = 1094.1 \pm 2.1\,(stat.) \pm 7.2\,(syst.) \pm 10.9\,(beam) \pm 12.7\,(lumi.)\mathrm{pb}$$

$$\sigma_{W^-\to\mu^-\nu} = 819.4 \pm 1.9\,(stat.) \pm 5.0\,(syst.) \pm 7.1\,(beam) \pm 9.5\,(lumi.)\mathrm{pb}$$

- Update on the $7\,\mathrm{TeV}$ measurement using $2\,\mathrm{fb}^{-1}$ of LHCb data;
- Results are consistent with the measurement of $Z \to ee$;
- Cross-section ratios are measured at sub-percent precision;
- The energy evolution is studied:
  - CoM energy ratios are presented;
  - Ratios of ratios are presented.

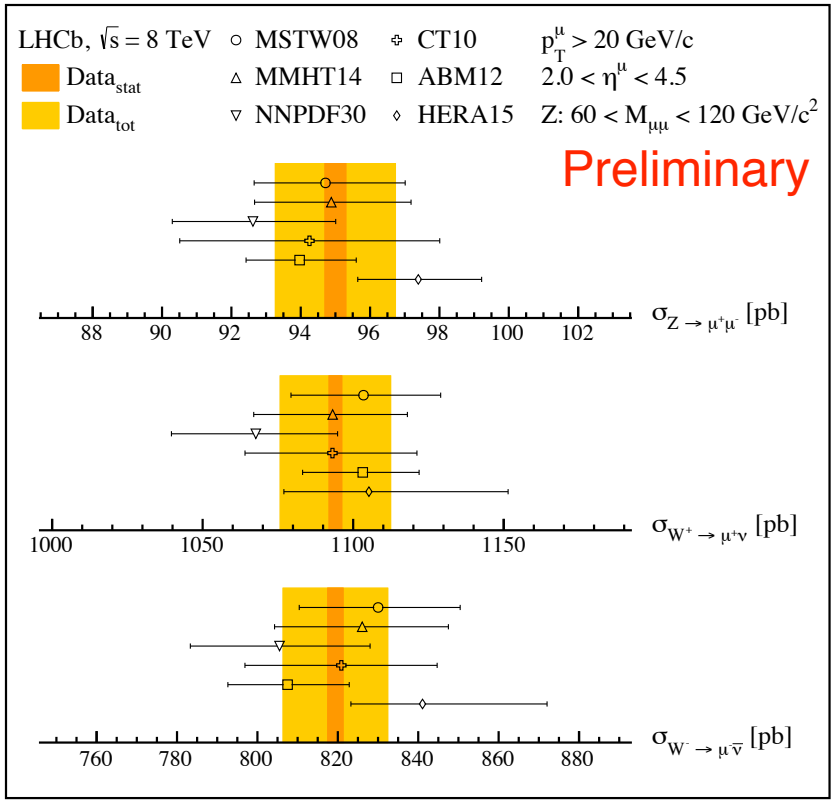

Inclusive W and Z @ 8 TeV differential cross-sections

LHCb-PAPER-2015-049

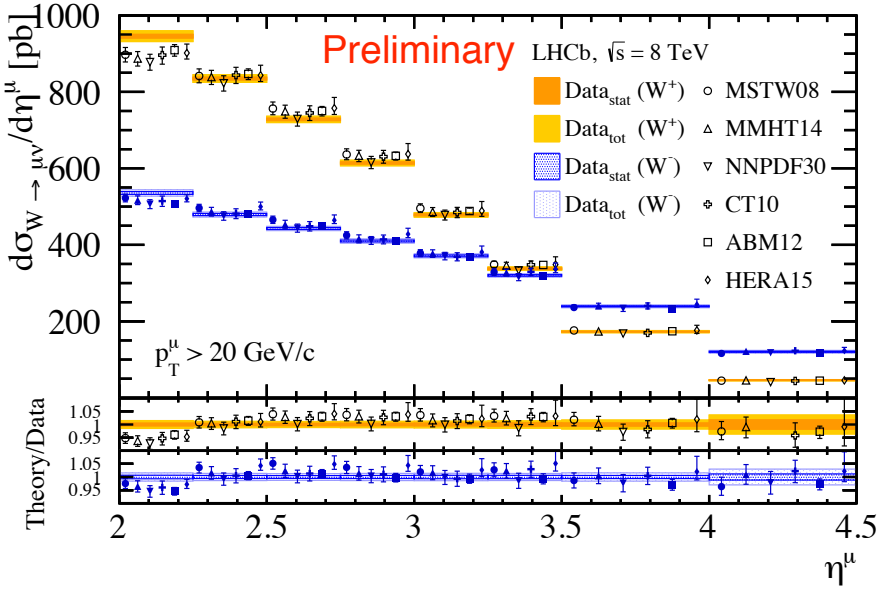

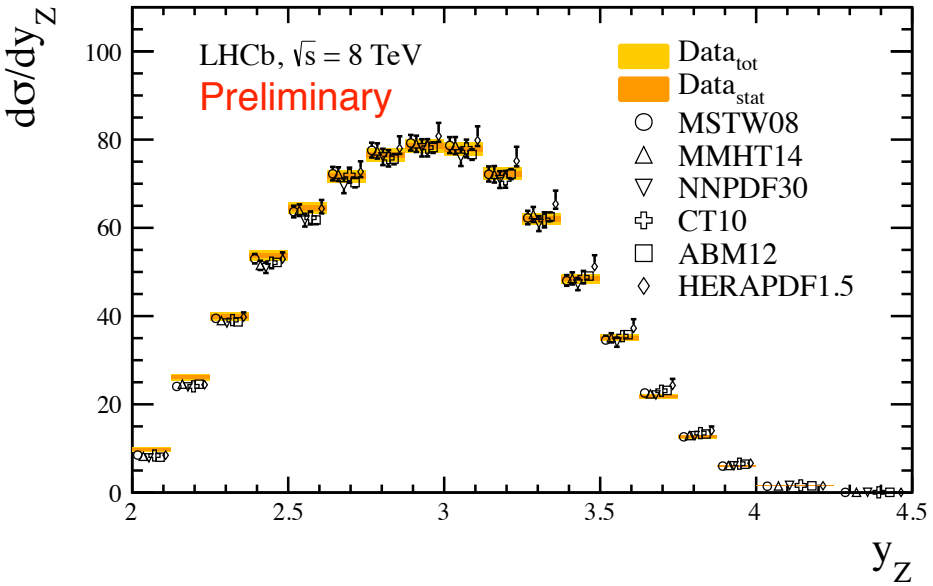

W and Z ratios @ 8 TeV

LHCb-PAPER-2015-049

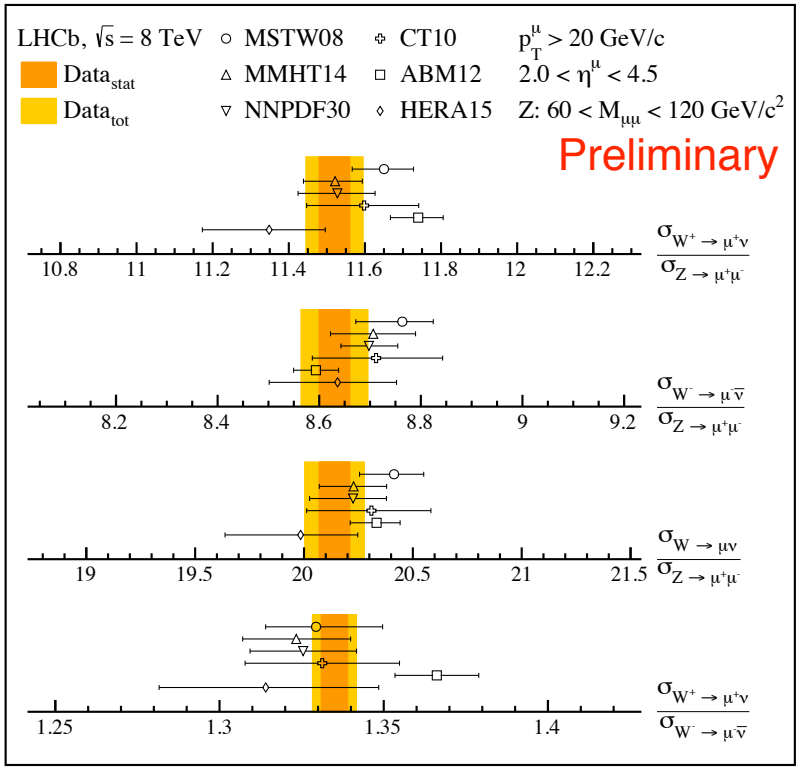

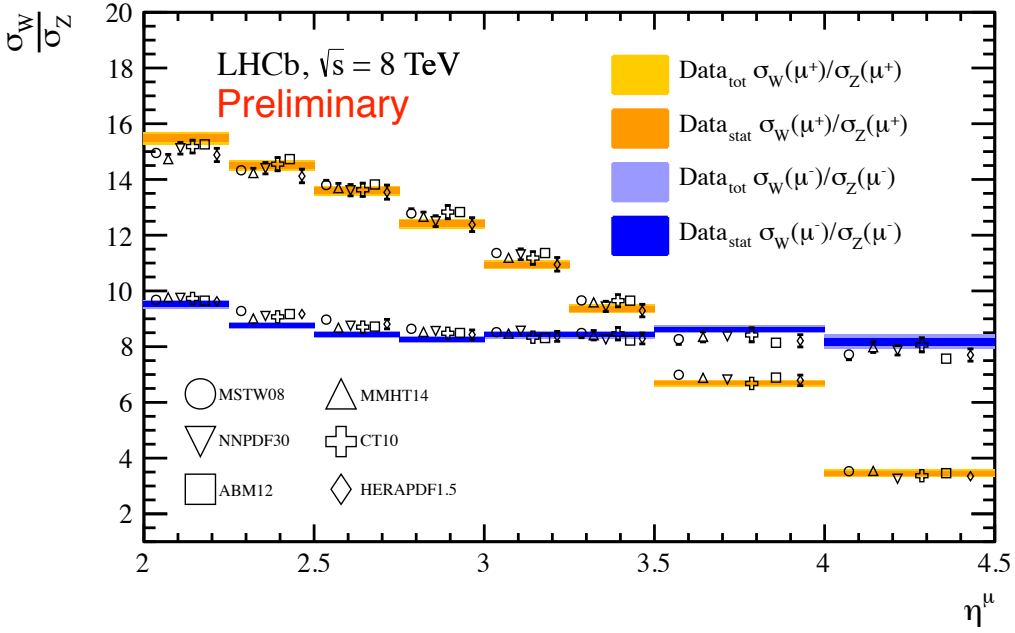

The differential $\sigma_W(\mu^-)/\sigma_Z(\mu^-)$ is flatter than the corresponding theory predictions.

Centre-of-mass ratios

LHCb-PAPER-2015-049

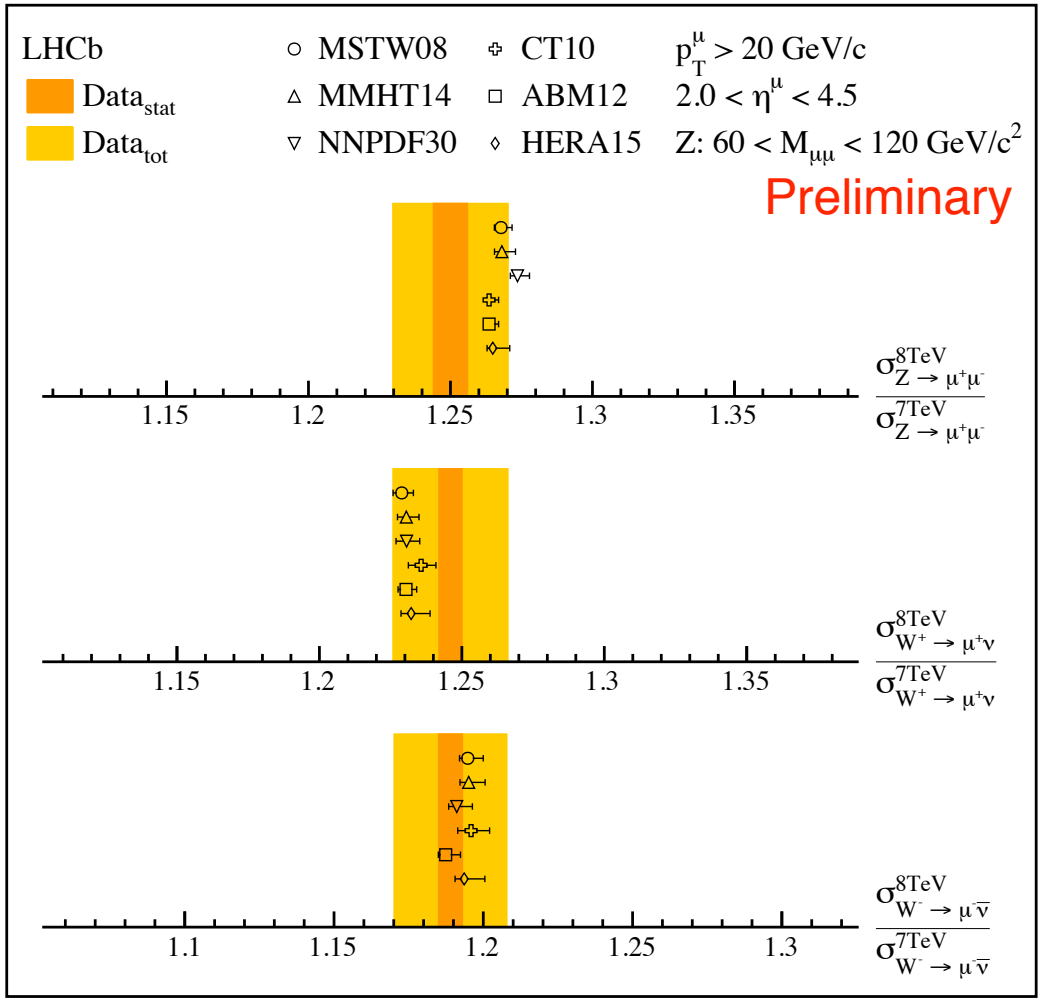

The luminosity is correlated between two years at the level of 0.55 and is accounted for.

Ratios of ratios

LHCb-PAPER-2015-049

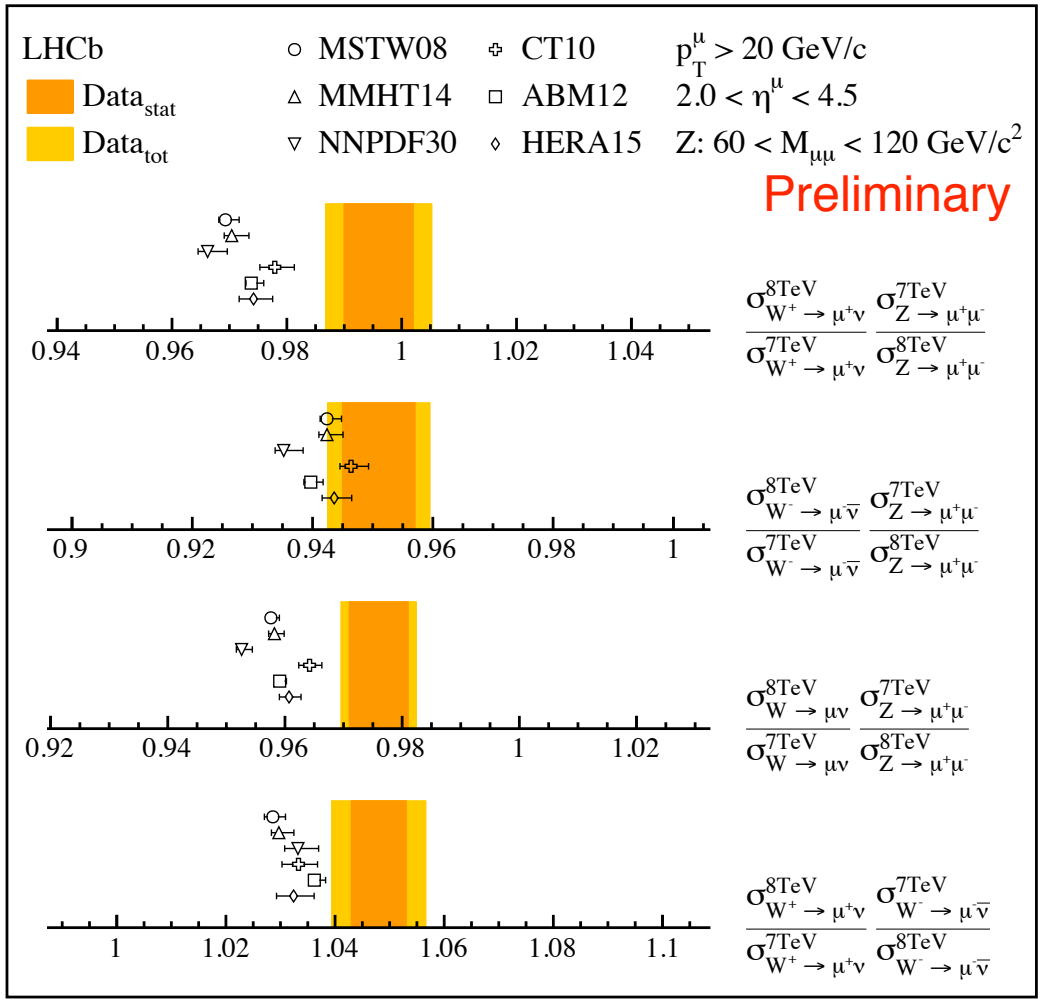

Ratios of ratios indicate mild tension with the theory predictions. However, they are correlated. The tension stems from the 7 TeV Z cross-section.

A_{FB} and the determination of the effective weak mixing angle

arXiv:1509.07645

- The forward-backward charge asymmetry for the process $Z/\gamma* \to \mu^+\mu^-$ is measured as a function of the invariant mass;
- Measured both at $7\,\mathrm{TeV}$ and at $8\,\mathrm{TeV}$, and combined.

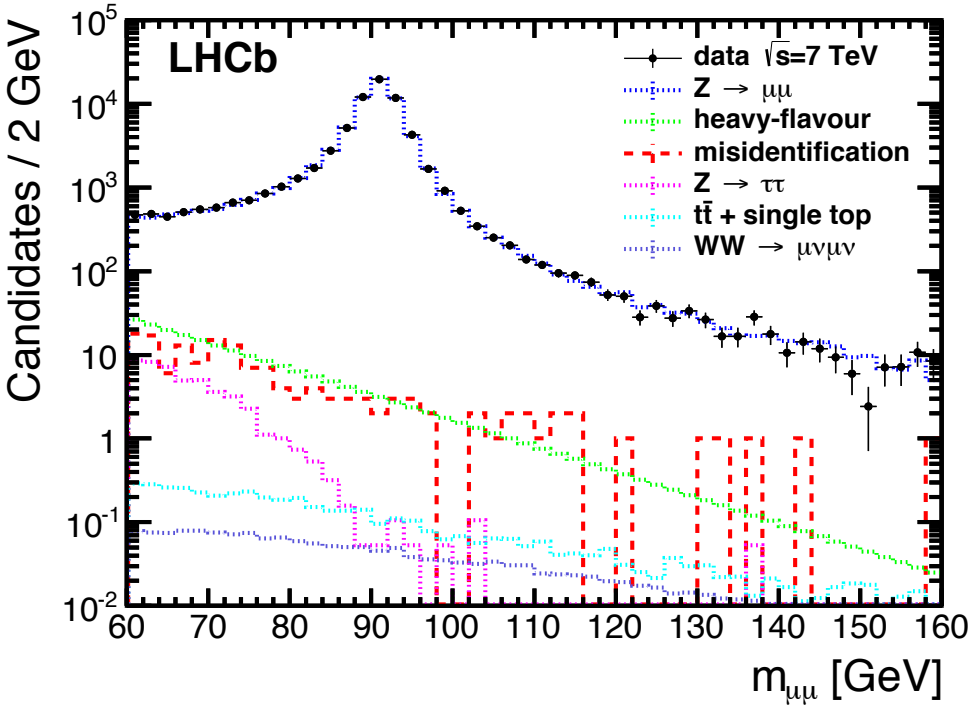

- Largest background contributions are:
- Semileptonic heavy-flavour decays;
- Misidentified hadrons;
- Hadrons decayed in flight.
- These are estimated using data-driven techniques.

A_{FB} and the determination of the effective weak mixing angle

arXiv:1509.07645

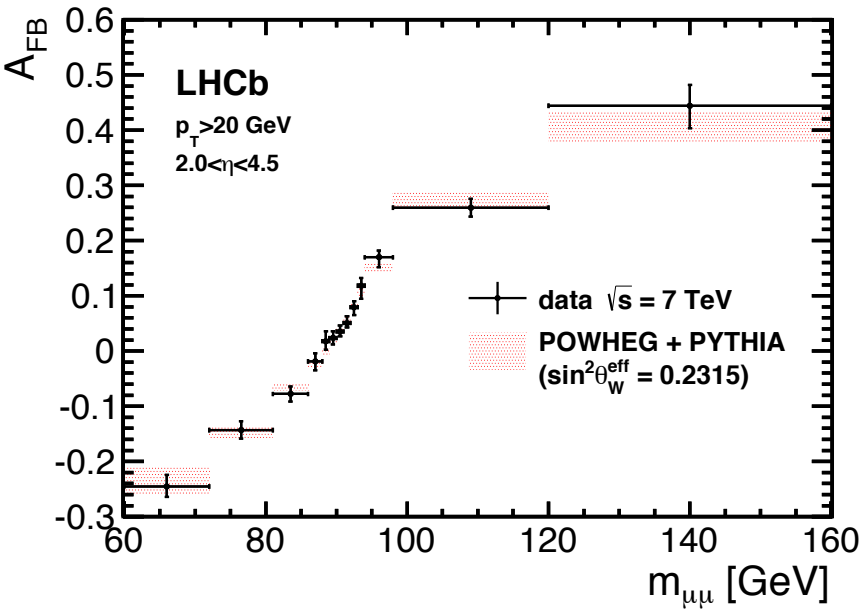

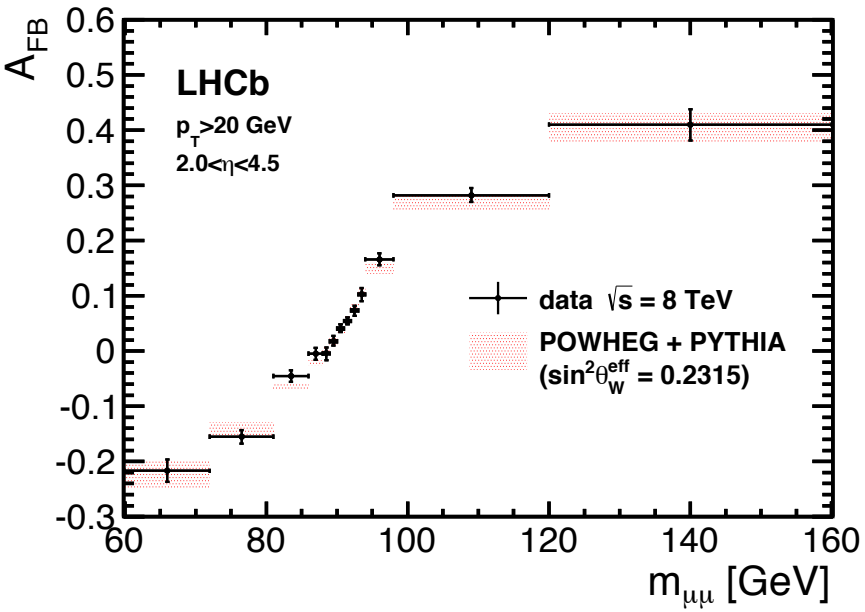

Corrections are applied to account for efficiencies, biases in the reconstructed momenta of the muons and differences in resolution between simulation and data.

A_{FB} and the determination of the effective weak mixing angle

arXiv:1509.07645

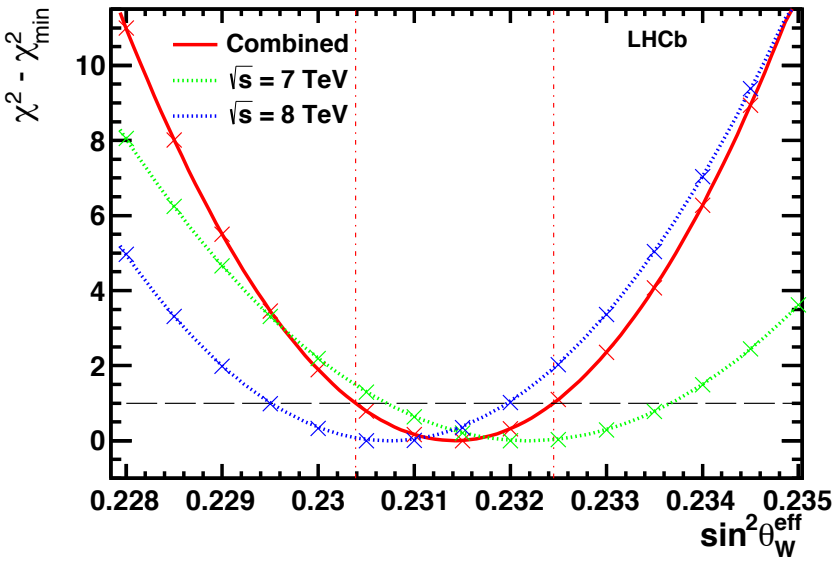

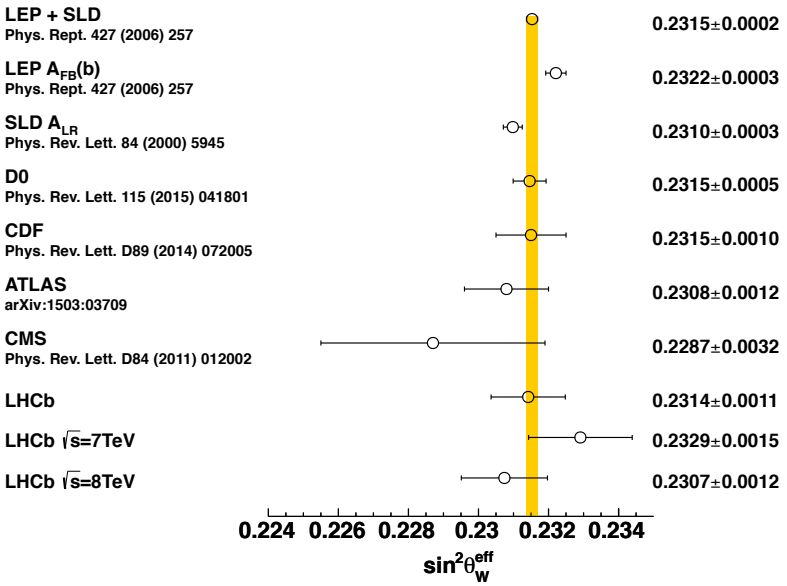

A_{FB}^{meas} is compared to the theoretical A_{FB}^{pred} for a range of $\sin^2\theta_W^{eff}$ values to extract the best-fit value. This result is in agreement with the current world average, and is one of the most precise determinations at hadron colliders to date.

A_{FB} – systematics

arXiv:1509.07645

Table 1: Weighted average of the absolute systematic uncertainties for A_{FB}, for different sources, given separately for $\sqrt{s} = 7$ and 8 TeV.

Source of uncertainty	$\sqrt{s} = 7\,\mathrm{TeV}$	$\sqrt{s} = 8\,\mathrm{TeV}$
curvature/momentum scale	0.0102	0.0050
data/simulation mass resolution	0.0032	0.0025
unfolding parameter	0.0033	0.0009
unfolding bias	0.0025	0.0025

Table 4: Weighted average of the absolute systematic uncertainties for $A_{\mathrm{FB}}^{\mathrm{pred}}$, for the different sources of theoretical uncertainty. The value quoted for the PDF uncertainty corresponds to the 68% confidence range, while for the others the maximum and minimum shifts are given. The correlations among the invariant mass bins are not taken into account.

Uncertainty	average $\Delta\lvert A_{\mathrm{FB}}^{\mathrm{pred}}\rvert$
PDF	0.0062
scale	0.0040
α_s	0.0030
FSR	0.0016

Top quark production at LHCb

Phys.Rev.Lett. 115,112001(2015)

σ_{top} is measured in the $W(\rightarrow \mu\nu) + b$ final state to be

$$\sigma_{top}[7\,\mathrm{TeV}] = 239 \pm 53\,(stat.) \pm 33\,(syst.) \pm 24\,(theory)\mathrm{fb}$$

$$\sigma_{top}[8\,\mathrm{TeV}] = 289 \pm 43\,(stat.) \pm 40\,(syst.) \pm 29\,(theory)\mathrm{fb}$$

- A significance of 5.4σ is achieved;
- Results are consistent with SM predictions;
- Test of BSM theories and N(N)LO calculations;
- Is sensitive to the gluon PDF.

$$p_T^{\mu} > 25\,\mathrm{GeV}$$
$$2.0 < \eta^{\mu} < 4.5$$
$$50 < p_T^{b-jets} < 100\,\mathrm{GeV}$$
$$2.2 < \eta^{b-jets} < 4.2$$
$$p_T^{\mu+b-jets} > 20\,\mathrm{GeV}$$

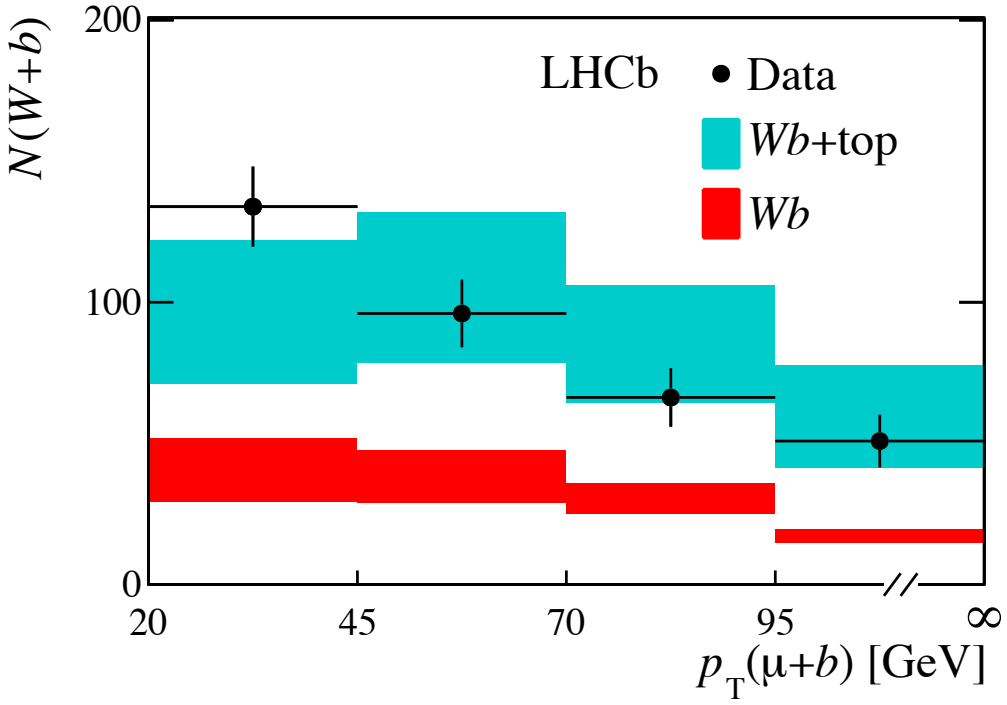

Exclusive Υ production

JHEP09(2015)084

Using $2.9\,\mathrm{fb}^{-1}$ of $7\,\mathrm{TeV}$ and $8\,\mathrm{TeV}$ data, exclusive $\Upsilon(1S)$ and $\Upsilon(2S)$ cross-sections are measured to be

$$\sigma(pp \to p\Upsilon(1S)p) = 9.0 \pm 2.1\,(stat.) \pm 1.7\,(syst.)\mathrm{pb}$$

$$\sigma(pp \to p\Upsilon(2S)p) = 1.3 \pm 0.8\,(stat.) \pm 0.3\,(syst.)\mathrm{pb}$$

- Results are consistent with SM predictions;
- An upper limit is set on the $\Upsilon(3S)$ cross-section;
- Measurement is sensitive to differences in (N)LO predictions, and theoretical modelling;
- Constrains the gluon PDF.

$$2.0 < y(\Upsilon) < 4.5$$
$$2.0 < \eta^{\mu} < 4.5$$

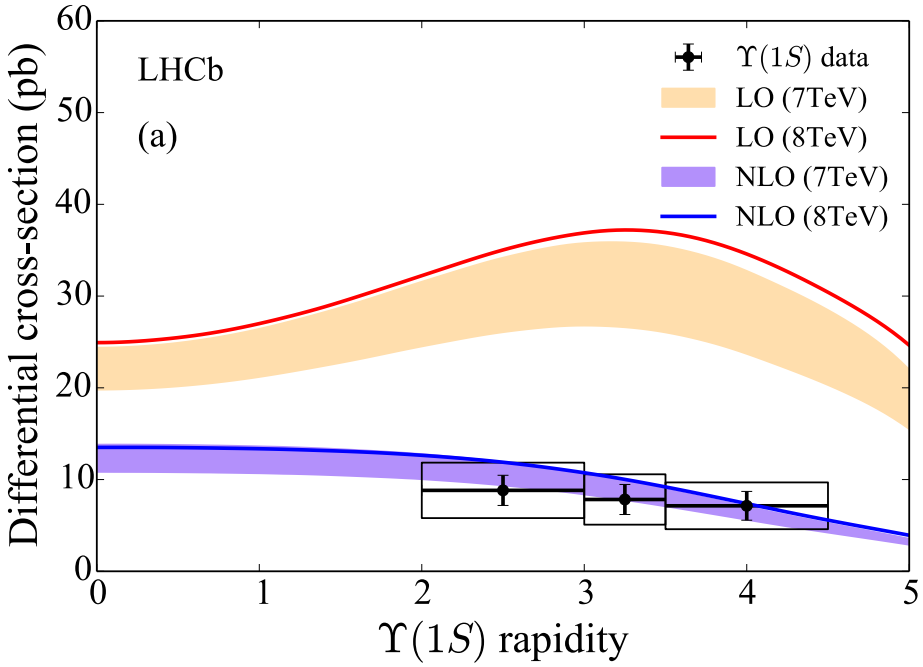

Summary and outlook

- LHCb continues to build on past successes in its electroweak program:
  - Most precise W and Z cross-section ratios at the LHC;
  - Novel centre-of-mass ratios are presented;
  - A precise determination of $\sin\theta_W$;
  - First observation of top quark production.
- Our measurements are seen to have an impact on PDFs;
- The higher energies of Run II will allow us to
  - probe lower values of x;
  - continue to investigate the energy evolution of electroweak boson production.

Appendix

LHCb phase space

While ATLAS&CMS are largely limited to $\eta \leq 2.5$ (with Bjorken-x in the range of $10^{-3} \leq x \leq 0.1$), LHCb detects W and Z daughters in $2 < \eta < 5$. These are formed in a highly boosted system with respect to the lab frame with one parton at $x_a \sim 0.1$ and the other at $x_b \sim 10^{-4}$.

$$y_{W(Z)} = \ln\left(\frac{x_a}{x_b}\right)^{\frac{1}{2}} \Longrightarrow x_{a,b} = \frac{M_{W(Z)}}{\sqrt{s}} e^{\pm y_{W(Z)}}$$

Motivation – ABM12

Phys. Rev. D 89 (2014) 054028

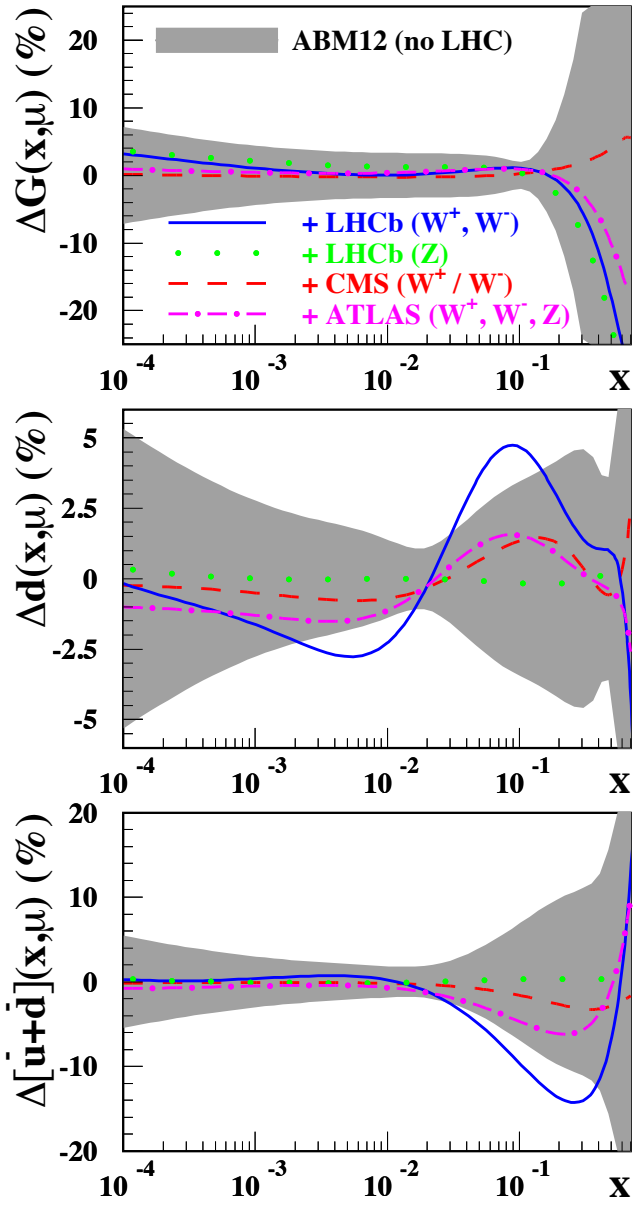

Early LHCb data of W production provide the largest impact on valence d and sea light quark PDFs.

Flavour decomposition of W

Eur. Phys. J. C 14 (2000) 133

- σ_W is sensitive to the flavour composition of the quark sea;
- Can be used in constraining the strange PDF.

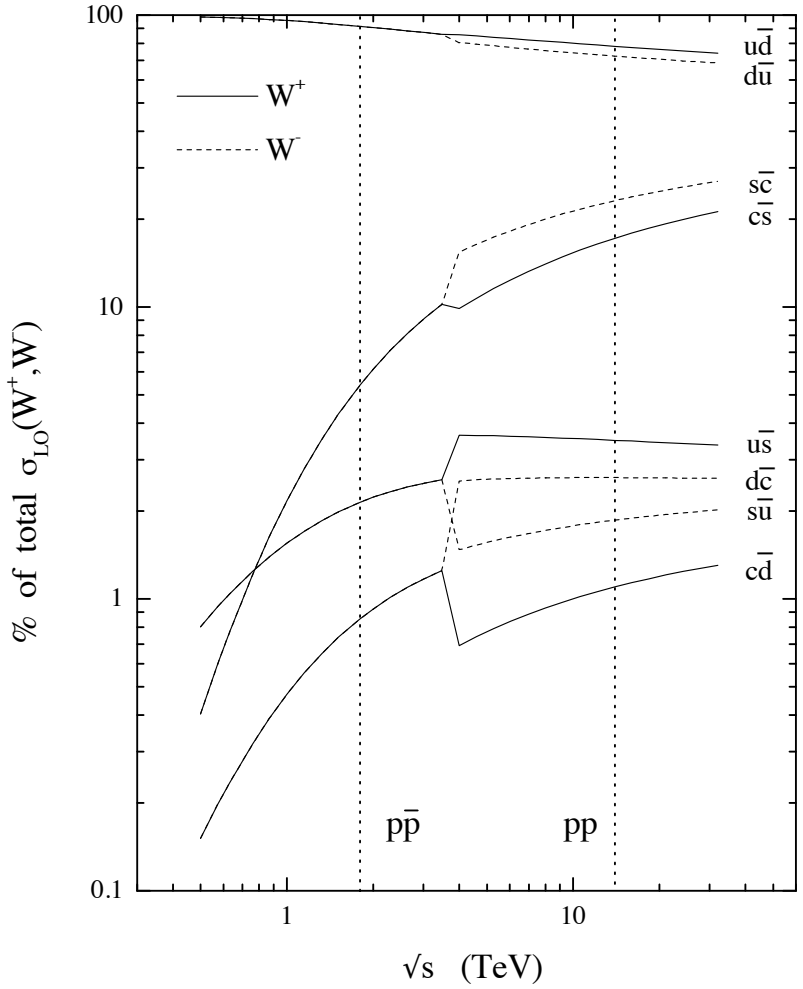

Charge asymmetry

Phys. Rev. D 69 (2004) 094008

The charge asymmetry is given as

$$\mathcal{A}(\eta_\ell) \equiv \frac{\frac{d\sigma^{W^+}}{d\eta_\ell} - \frac{d\sigma^{W^-}}{d\eta_\ell}}{\frac{d\sigma^{W^+}}{d\eta_\ell} + \frac{d\sigma^{W^-}}{d\eta_\ell}} \approx \frac{u-d}{u+d} \approx \frac{u_{val} - d_{val}}{u_{val} + d_{val} + 2u_{sea}}$$

- $\mathcal{A}(\eta_\ell)$ is almost completely insensitive to higher order QCD corrections;
- several experimental uncertainties also cancel;
- a measurement of this quantity is a powerful probe of PDFs.

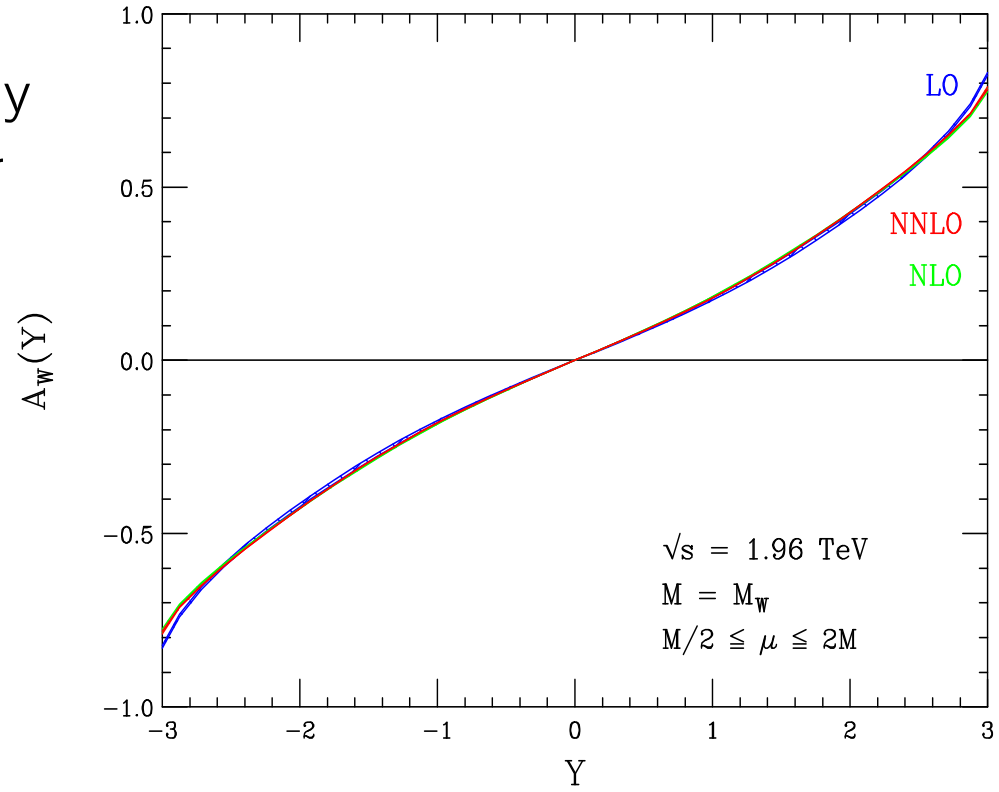

Inclusive Z – systematics

JHEP08(2015)039

Source	Uncertainty (%)
Statistical	0.39
Trigger efficiency	0.07
Identification efficiency	0.23
Tracking efficiency	0.53
FSR	0.11
Purity	0.22
GEC efficiency	0.26
Systematic	0.68
Beam energy	1.25
Luminosity	1.72
Total	2.27

Source	Uncertainty (%)			
	R_{WZ}	R_{W^+Z}	R_{W^-Z}	R_W
Statistical	0.45	0.48	0.50	0.38
Trigger efficiency	0.15	0.16	0.13	0.07
Identification efficiency	0.12	0.12	0.12	0.03
Tracking efficiency	0.24	0.23	0.26	0.08
FSR	0.16	0.21	0.17	0.21
Purity	0.41	0.49	0.55	0.62
GEC efficiency	0.27	0.28	0.29	0.18
Systematic	0.60	0.67	0.72	0.69
Beam energy	0.26	0.19	0.34	0.15
Total	0.79	0.85	0.94	0.80

Inclusive W – results

JHEP12 (2014) 079

$\sigma_{W\to\mu\nu}$ cross-section at $7\,\mathrm{TeV}$ is measured to be

$$\sigma_{W^+\to\mu^+\nu} = 878.0 \pm 2.1\,(stat.) \pm 6.7\,(syst.) \pm 15.0\,(lumi.)\mathrm{pb}$$

$$\sigma_{W^-\to\mu^-\nu} = 689.5 \pm 2.0\,(stat.) \pm 5.3\,(syst.) \pm 11.8\,(lumi.)\mathrm{pb}$$

The cross-section ratio is measured to be

$$\frac{\sigma_{W^+\to\mu^+\nu}}{\sigma_{W^-\to\mu^-\nu}} = 1.274 \pm 0.005\,(stat.) \pm 0.009\,(syst.) \pm 0.002\,(beam)$$

- Results are given at Born-level;
- Theory prediction is from FEWZ at NNLO;
- A selection of NNLO PDF sets are used.

$$p_{\mathrm{T}}^{\mu} > 20\,\mathrm{GeV}$$
$$2.0 < \eta^{\mu} < 4.5$$

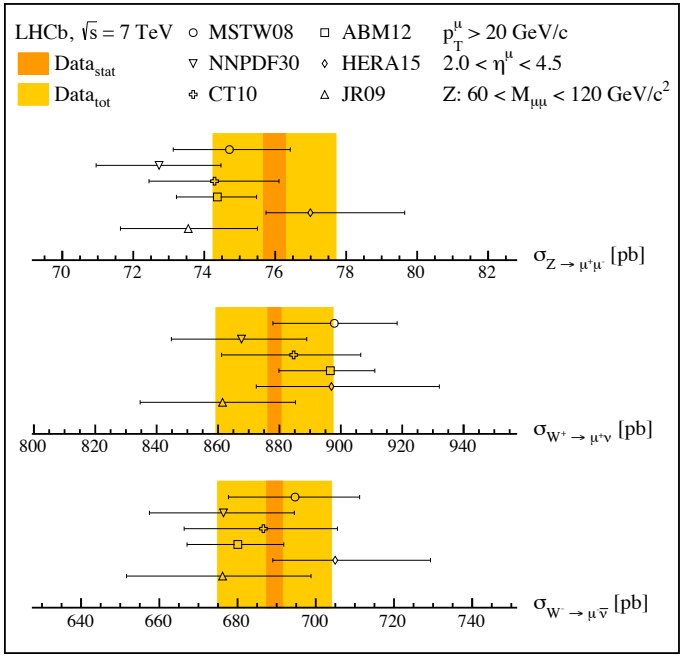

Inclusive W – differential cross-sections

JHEP12 (2014) 079

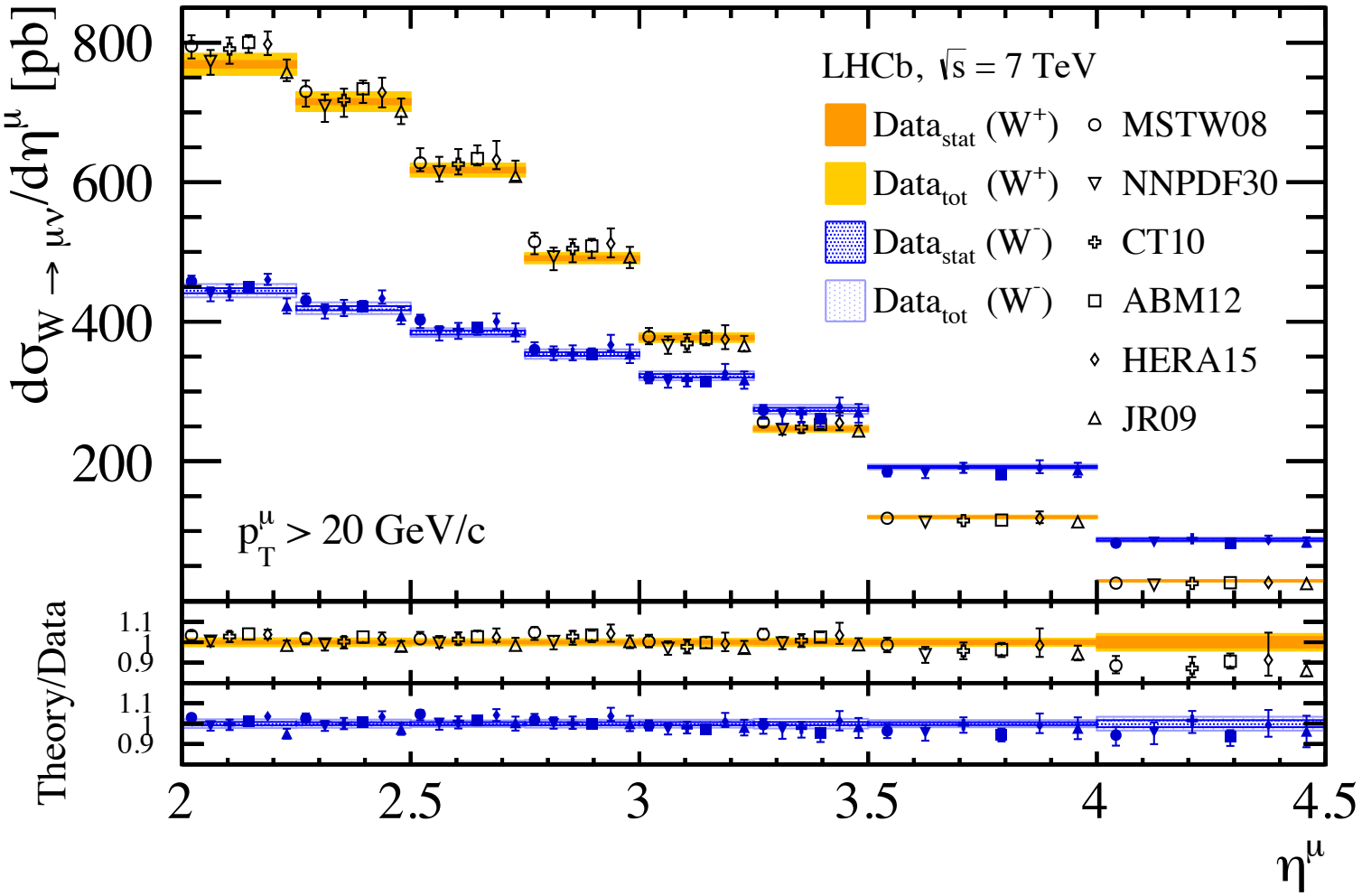

Inclusive W – cross-section ratio and the charge asymmetry

JHEP12 (2014) 079

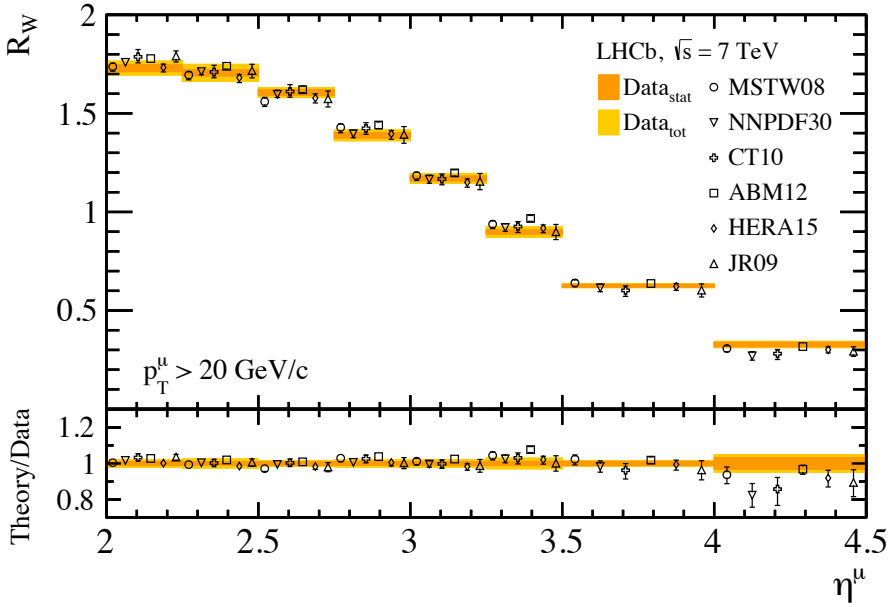

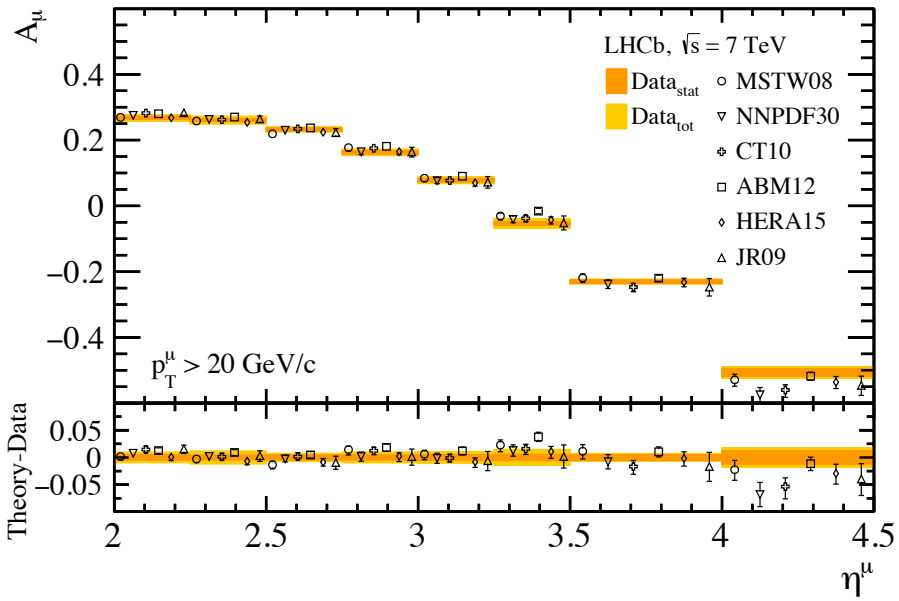

$$R(\eta_\ell) \equiv \frac{\frac{d\sigma^{W^+}}{d\eta_\ell}}{\frac{d\sigma^{W^-}}{d\eta_\ell}}$$

$$\mathcal{A}(\eta_\ell) \equiv \frac{\frac{d\sigma^{W^+}}{d\eta_\ell} - \frac{d\sigma^{W^-}}{d\eta_\ell}}{\frac{d\sigma^{W^+}}{d\eta_\ell} + \frac{d\sigma^{W^-}}{d\eta_\ell}}$$

The measured cross-sections are in agreement with NNLO predictions using different PDF sets.

Inclusive W – comparison to ATLAS

JHEP12 (2014) 079

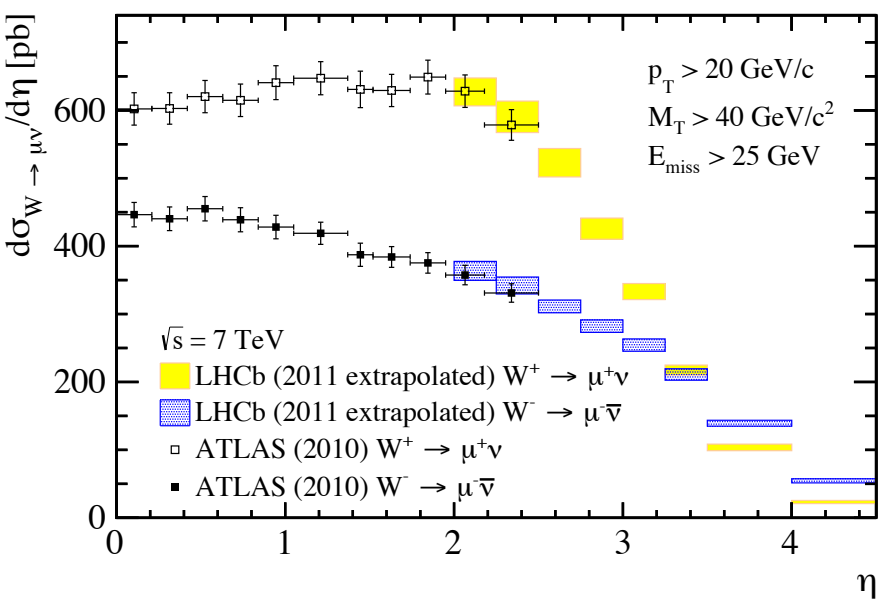

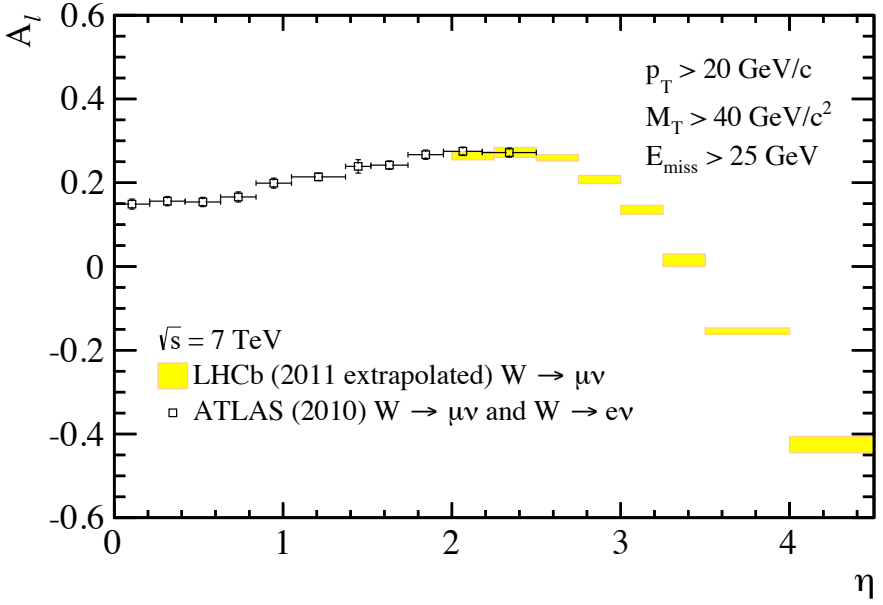

Inclusive W/Z cross-sections at LHCb are complementary to ATLAS (and also to CMS).

Inclusive W – systematics

JHEP12 (2014) 079

Table 1: Summary of the systematic uncertainties on the inclusive cross-sections and their ratio.

Source	$\Delta\sigma_{W^+\to\mu^+\nu}$ [%]	$\Delta\sigma_{W^-\to\mu^-\overline{\nu}}$ [%]	ΔR_W [%]
Template shape	0.28	0.39	0.59
Template normalisation	0.10	0.10	0.06
Reconstruction efficiency	1.21	1.20	0.12
Selection efficiency	0.33	0.32	0.18
Acceptance and FSR	0.18	0.12	0.21
Luminosity	1.71	1.71	—

Inclusive W and Z @ $8\,\mathrm{TeV}$– systematics

LHCb-PAPER-2015-049

Source	Uncertainty (%)		
	σ_{W^+}	σ_{W^-}	σ_Z
Statistical	0.19	0.23	0.27
Purity	0.28	0.21	0.21
Tracking	0.26	0.24	0.48
Identification	0.11	0.11	0.21
Trigger	0.14	0.13	0.05
GEC	0.40	0.41	0.34
Selection	0.24	0.23	—
Acceptance	0.08	0.08	—
FSR	0.14	0.11	0.13
Momentum scale	0.05	0.12	—
Systematic	0.65	0.62	0.67
Beam energy	1.00	0.86	1.15
Luminosity	1.16	1.16	1.16
Total	1.67	1.59	1.79

Inclusive W and Z @ $8\,\mathrm{TeV}$– systematics

LHCb-PAPER-2015-049

Source	Uncertainty (%)			
	$R_{W^\pm}$	R_{W^+Z}	R_{W^-Z}	R_{WZ}
Statistical	0.30	0.31	0.33	0.36
Purity	0.25	0.28	0.21	0.22
Tracking	0.06	0.22	0.24	0.23
Identification	0.01	0.11	0.11	0.11
Trigger	0.04	0.10	0.09	0.09
GEC	0.13	0.21	0.22	0.21
Selection	0.10	0.24	0.23	0.23
Acceptance	0.11	0.21	0.19	0.17
FSR	0.18			
Momentum scale	0.07	0.05	0.12	0.08
Systematic	0.38	0.55	0.52	0.50
Beam energy	0.14	0.15	0.29	0.21
Total	0.50	0.65	0.68	0.65

Inclusive W and Z @ $8\,\mathrm{TeV}$– systematics

LHCb-PAPER-2015-049

Source	Uncertainty (%)						
	$R^{8/7}_{W^+}$	$R^{8/7}_{W^-}$	$R^{8/7}_{Z}$	$R^{8/7}_{R_{WZ}}$	$R^{8/7}_{R_{W^+Z}}$	$R^{8/7}_{R_{W^-Z}}$	$R^{8/7}_{R_{W^\pm}}$
Statistical	0.30	0.37	0.49	0.55	0.58	0.62	0.48
Purity	0.41	0.45	—	0.29	0.41	0.45	0.65
Tracking	0.33	0.27	0.53	0.24	0.23	0.26	0.09
Identification	0.07	0.07	0.13	0.07	0.07	0.06	0.03
Trigger	0.27	0.25	0.09	0.17	0.19	0.16	0.08
GEC	0.15	0.14	0.09	0.08	0.09	0.09	0.07
Selection	0.12	0.17	—	0.16	0.17	0.17	0.04
Acceptance/FSR	0.05	0.06	0.04	0.06	0.07	0.07	0.08
Momentum scale	0.05	0.12	—	0.08	0.05	0.12	0.07
Systematic	0.64	0.64	0.56	0.47	0.55	0.60	0.66
Beam energy	0.06	0.05	0.10	0.05	0.04	0.05	—
Luminosity	1.45	1.45	1.45	—	—	—	—
Total	1.61	1.62	1.63	0.73	0.80	0.86	0.82

Top – systematics

Phys.Rev.Lett. 115,112001(2015)

Table 1: Relative systematic uncertainties. The symbol † denotes an uncertainty that only applies to the cross-section measurement and not the significance determination. Only the luminosity uncertainty depends on $\sqrt{s}$: 2% at 7 TeV and 1% at 8 TeV.

source	uncertainty
GEC	2%
$p_{\mathrm{T}}(\mu)/p_{\mathrm{T}}(j_\mu)$ templates	5%
jet reconstruction	2%
SV-tag BDT templates	5%
b-tag efficiency	10%
trigger & μ selection	2%†
jet energy	5%†
$W \to \tau \to \mu$	1%†
luminosity	1–2%†
Total	14%
Theory	10%

Upsilon – mass fit

JHEP09(2015)084

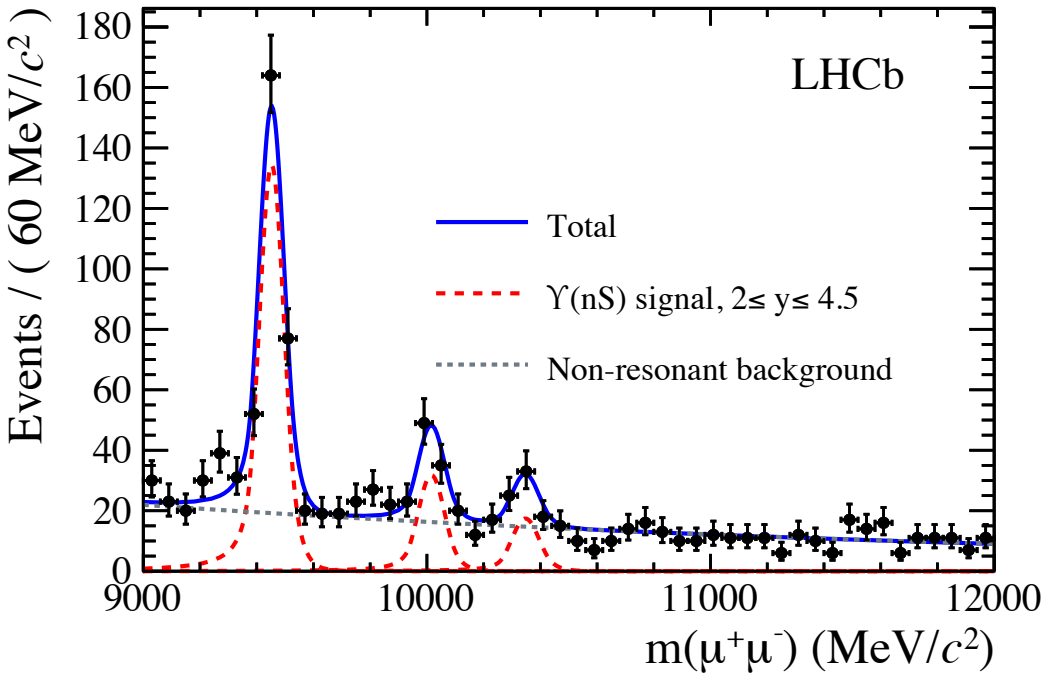

Figure 2: Invariant dimuon mass spectrum for 7 TeV and 8 TeV data in the rapidity range $2 < y(\Upsilon) < 4.5$ (black points). The fit PDF is superimposed (solid blue line). The $\Upsilon(1S, 2S, 3S)$ signal components, used to derive weights, are indicated with a long-dashed (red) line, and the non-resonant background is marked with a short-dashed (grey) line.

Upsilon – p_T^2 fit

JHEP09(2015)084

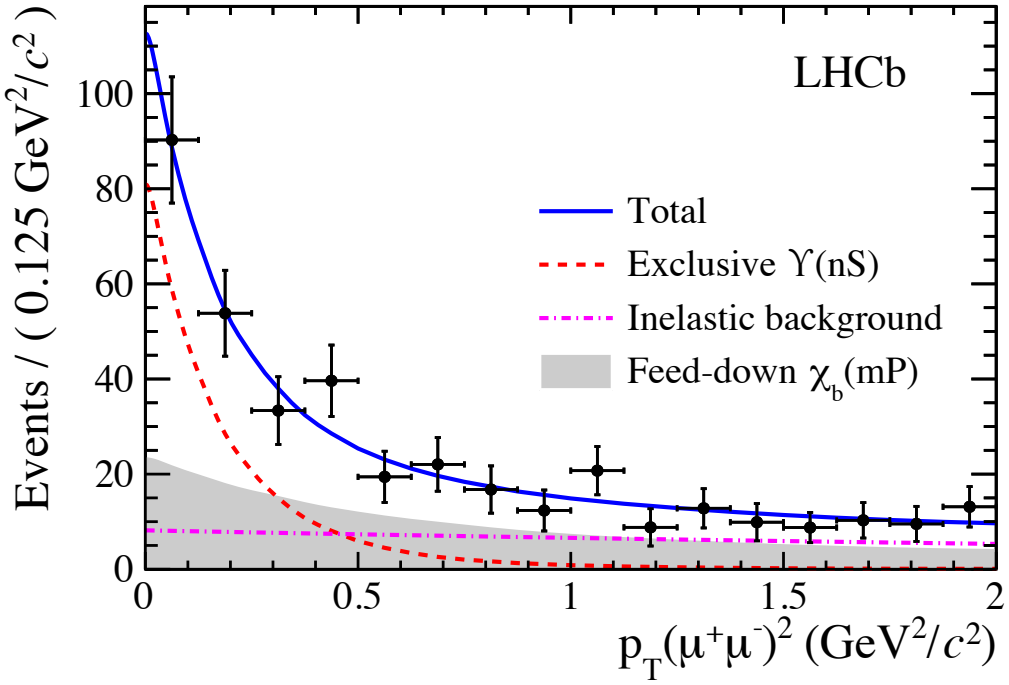

Figure 3: Fit to the p_{T}^2 distribution of the Υ candidates in the full rapidity range.

Upsilon – systematics

JHEP09(2015)084

Table 3: Summary of the relative systematic uncertainties, in %.

	$2 < y < 3$	$3 < y < 3.5$	$3.5 < y < 4.5$	$2 < y < 4.5$		
	$\Upsilon(1S)$	$\Upsilon(1S)$	$\Upsilon(1S)$	$\Upsilon(1S)$	$\Upsilon(2S)$	$\Upsilon(3S)$
Purity fit	14.2	14.2	14.2	13.7	13.7	13.7
Feed-down b.g.	12.2	12.2	12.3	12.2	14.6	12.5
Υ' feed-down	4.0	4.3	5.4	4.5	11.1	–
Mass fit	2.2	2.8	2.9	2.1	2.8	3.6
Luminosity	2.3	2.3	2.3	2.3	2.3	2.3
$\mathcal{B}(\Upsilon \to \mu^+\mu^-)$	2.0	2.0	2.0	2.0	8.8	9.6
Total	19.5	19.7	20.0	19.3	24.8	21.4